Bone-Tissue Interface

Jiang Du, Ph.D.
Associate Professor, Department of Radiology
University of California, San Diego

1. Introduction

Bone is a composite material consisting of mineral (~45% by volume), organic matrix (~30%) and water (~25%) [1]. It is of central importance to image bone as well as bone-tissue interface. In this lecture, I will introduce novel magnetic resonance imaging (MRI) techniques to image bone and bone-tissue interface including periosteum and calcified cartilage – an interface between bone and articular cartilage.

2. Bone Imaging

In recent years various types of ultrashort echo time (UTE) pulse sequences have been developed to directly detect signal from bone using clinical MR scanners [2-8]. The different water components in cortical bone, including bulk water residing in the macroscopic pores and water loosely bound to the organic matrix can now be selectively imaged with different UTE or clinical sequences. **Figure 1** shows a representative cortical bone sampled imaged with 2D fast spin echo (FSE), 2D gradient recalled echo (GRE), 2D and 3D UTE, and 2D and 3D adiabatic inversion recovery prepared UTE (IR-UTE). Bulk water residing in the pores of cortical bone is visible with FSE but not GRE sequences, consistent with its long T2, but short T2*. The 2D and 3D UTE sequences detect both bulk water in the pores (high signal fine structure) and water bound to the organic matrix (uniform background signal). The 2D/3D IR-UTE images show only uniform background signal corresponding to water bound to the matrix, with fine structure disappearing because the bulk water signal is suppressed by the adiabatic inversion pulse. A variety of quantitative bone imaging techniques (bound/pore water quantification as well as measurements of T1, T2*, magnetization transfer ratio or MTR) will also be discussed in this lecture.

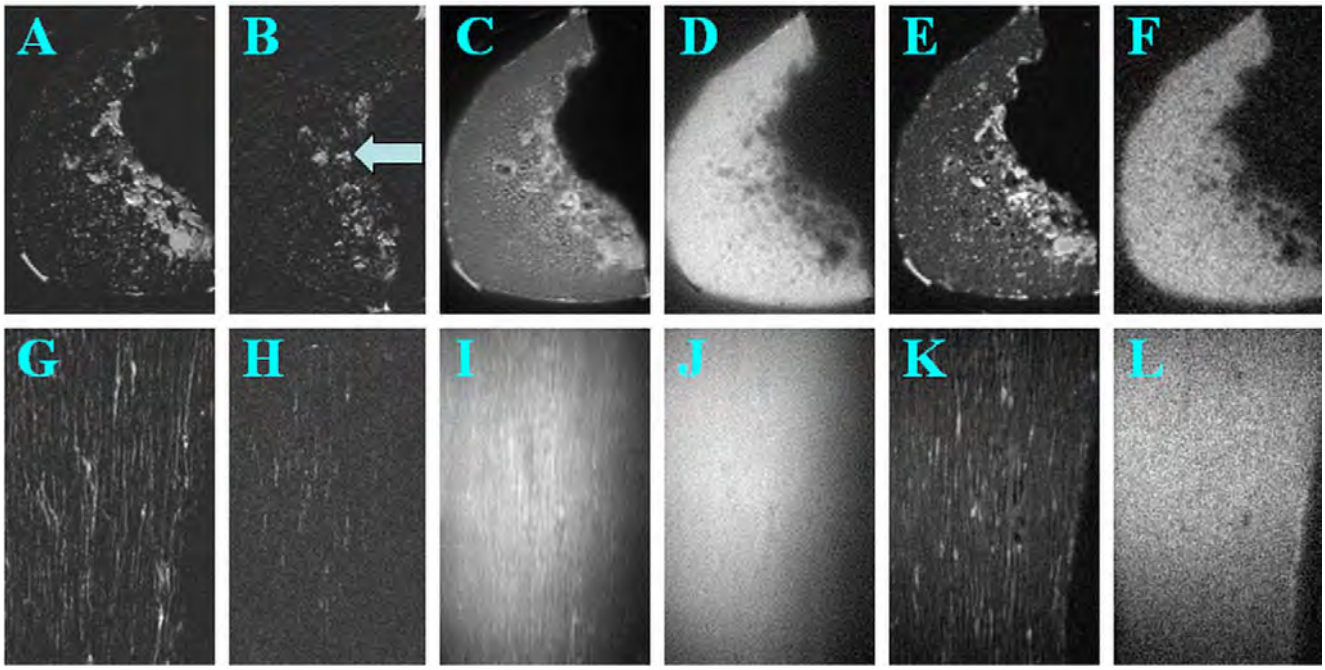

Figure 1. Axial (1st row) and sagittal (2nd row) imaging of a cortical bone sample with 2D FSE (A, G), 2D GRE (B, H), 2D UTE (C, I), 2D IR-UTE (D, J), 3D UTE (E, K) and 3D IR-UTE (F, L) sequences. Free water in the Haversian canals is detected by both FSE, 2D and 3D UTE sequences. 2D and 3D IR-UTE images show a relatively uniform bright signal, consistent with only bound water being detected. GRE image show little signal for bound and free water in cortical bone. The bright signal in (B) corresponds to marrow fat (arrow).

3. Periosteum Imaging

The periosteum plays a key role in bone nutrition and fracture healing [9]. The 2D UTE sequence was combined with a maximal phase 90^0 pulse followed by gradient dephasing to suppress long T2 signals from muscle and fat. This approach provides high signal for both bone and periosteum, but with low contrast between these two tissues. We employed a variable TE (TE varied from 8 to 1000 μs) acquisition strategy, resulting in a relatively long effective TE. At longer TEs only high signal from periosteum was left, while signals from cortical bone decayed to zero. **Figure 2** shows an image of periosteum. The following acquisition parameters were used: FOV = 10 cm, 5 mm thick, TR = 40 ms, TE = 8 μs, flip angle = 60°, BW = ±62.5 kHz, number of projections = 2025 (interleaved into 27 groups with TE delay of 40 μs per interleave), readout = 512 and 256, respectively, scan time = 8 minutes. Periosteum was selectively depicted with excellent image contrast.

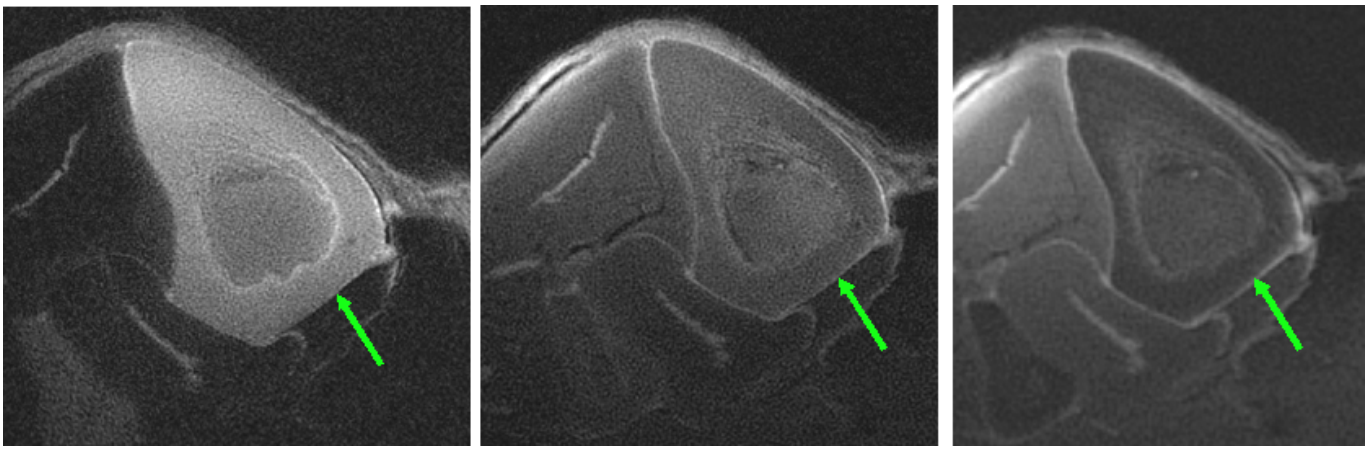

Figure 2. Periosteum imaging using conventional UTE acquisition (left) and variable TE UTE acquisition with a readout of 512 (middle) and 256 (right), which generate high contrast images of periosteum (green arrow).

T2* of periosteum can be measured by using long T2 suppressed UTE acquisitions at a series of TE delays. Preliminary study shows a short T2* of ~4 ms for normal periosteum, as shown in the following **Figure 3**.

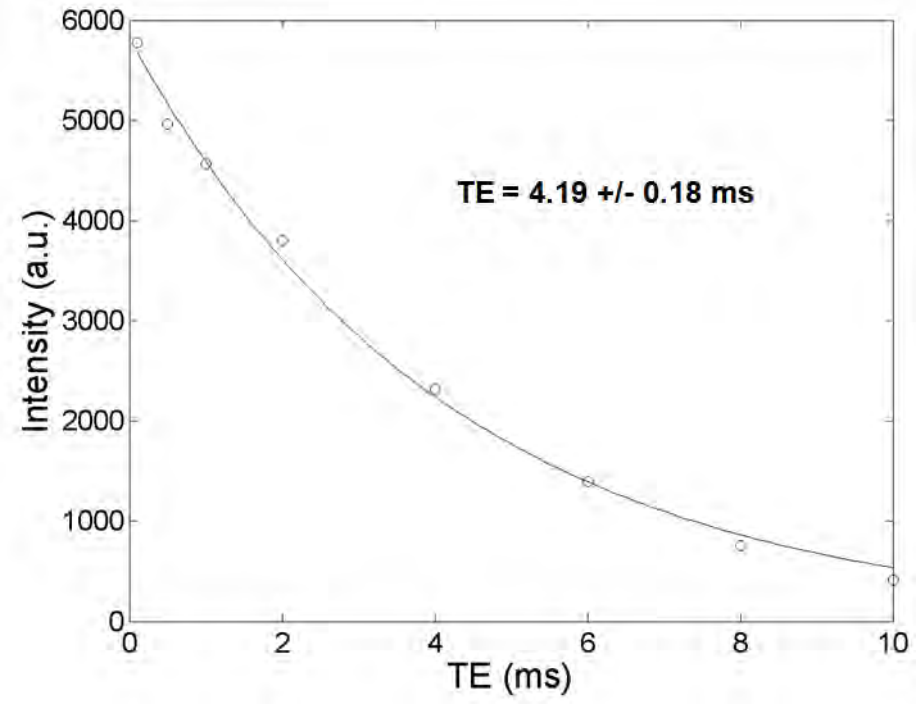

Figure 3. Single component fitting of UTE images shows a short T2* of 4.19 ± 0.18 ms for periosteum.

4. Calcified Cartilage Imaging

Calcified cartilage is the interface between subchondral bone and articular cartilage [10]. One of the most important questions about calcified cartilage is its involvement in the initial of pathogenesis in osteoarthritis (OA). It is generally believed that the initial changes of OA occur in the noncalcified part of the cartilage rather than the calcified layer, and that degeneration and erosion of the articular cartilage result in mechanical overload. Bone responds by becoming sclerotic, and this leads to further degeneration [11]. However, a number of recent studies have found changes in calcified cartilage and subchondral bone (SCB) that are not readily explicable with this model [12-18]. Calcified cartilage is an order of magnitude less stiff than bone, but 10-100 fold stiffer than cartilage [13]. This supports the concept that calcified cartilage forms a transitional zone of intermediate stiffness between the more superficial articular cartilage and SBC. In adults calcified cartilage becomes quiescent but not inactive. In OA calcified cartilage may be reactive and progressively extend to and calcify adjacent unmineralized cartilage. This may contribute to relative thinning of uncalcified cartilage and an increase in the force gradient across uncalcified cartilage leading to more damage [14]. Burr found that in OA calcified cartilage was significantly denser and had significantly more mineral than the adjacent SCB [15]. He concluded that it was likely that changes in the mineral content and thickness of calcified cartilage played a greater role in the pathogenesis of OA than had previously been realized. Ferguson et al studied calcified cartilage and SCB in normal and osteoarthritic human femoral heads and found that calcified cartilage was hypermineralized and twice as hard as neighboring SCB [16]. Very highly mineralized cartilage fragments may function as a grinding abrasive, accelerating wear rates whether attached to, or separated from the bony surface of calcified cartilage. Highly mineralized regions can also alter loading patterns and thereby contribute to further destruction of the joint tissues [16]. Revell et al were able to recover joints at the time of surgery from 50 patients with OA and concluded that calcified cartilage was active in OA [17]. Histological studies have also revealed the presence of multiple tidemarks coupled with thickening and over-mineralization of calcified cartilage in the OA joint [18].

Taken together, the results of different studies show that calcified cartilage may contribute to OA via altered growth plate-like behavior of the deep cells of the deep zone and bony remodeling. In addition a number of age-correlated changes in calcified cartilage can compromise adjacent noncalcified cartilage and cause it to degenerate. Thus calcified cartilage may play an important role in the initiation and/or progression of OA. The study of early and late alterations to calcified cartilage may therefore be important in elucidating the structural and functional pathogenesis of OA including features associated with the internal stages of the disease.

In recent years, several types of UTE sequences have been developed for high resolution morphological imaging of calcified cartilage [19, 20]. Quantitative UTE imaging sequences have also been developed to measure T1 [21], T1rho [20] and T2* [20, 22, 23] in the different layers of articular cartilage.

4.1 Morphological UTE Imaging of Calcified Cartilage

4.1.1 Multi-echo UTE Imaging of Articular Cartilage

Multi-echo acquisitions followed by later echo subtraction has been shown to be effective in suppressing long and medium T2 signals and providing high contrast imaging of short T2 components in the brain, knee and cortical bone at 1.5T [2]. This is achieved by subtracting the later echo image from the first one, equivalent to band pass filtering. Short T2 signals decay to zero or near zero by the time of the second echo and are thus minimally affected by the subtraction. Signals from fat may reduce the conspicuity and dynamic range of the short T2 signals from the deep layers of cartilage. As a consequence fat suppression techniques are typically applied in an effort to increase the dynamic range of the deep layers of cartilage and thereby improve their contrast with surrounding tissues. **Figure 4** shows dual echo images of a cadaveric knee sample with fat saturation. Excellent image contrast is achieved for calcified cartilage in the subtracted image (arrows). The combination of fat saturation and dual echo gradient echo subtraction suppresses both fat and long T2 water signals simultaneously.

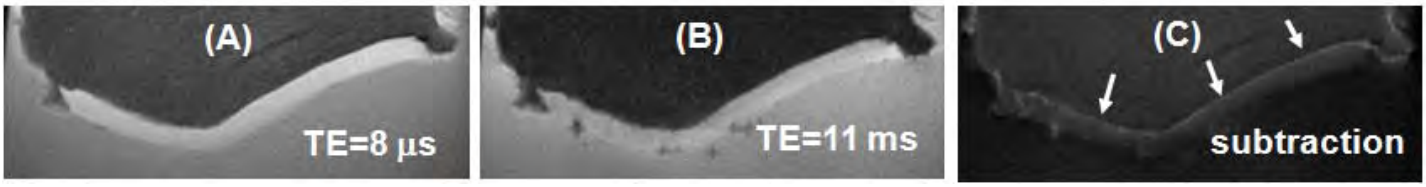

Figure 4. Fat suppressed dual echo UTE imaging of a cadaveric patella sample with a TE of 8 μs (A) and 11 ms (B). The imaging FOV of 8 cm, readout of 512, and slice thickness of 1.7 mm result in an acquired voxel size of 0.156×0.156×1.7 mm^3, providing excellent depiction of the deep layers of cartilage with high contrast on the subtraction image (arrows in C).

4.1.2 Dual Inversion Recovery UTE (DIR-UTE) Imaging of Articular Cartilage

In DIR-UTE imaging two long adiabatic inversion recovery pulses are employed to suppress long T2 signals from the superficial layers of articular cartilage as well as from marrow fat [19, 20]. The first adiabatic inversion pulse (duration ~ 25 ms, spectral bandwidth ~ 500 Hz) is centered near the water peak and has an inversion time of TI_1 to invert and null the longitudinal magnetization of the superficial layers of articular cartilage. The second adiabatic inversion pulse which is of the same duration and spectral bandwidth, is centered near the fat peak and has an inversion time of TI_2 to invert and null the longitudinal magnetization of marrow fat. The superficial layers of cartilage have longer T1s than marrow fat, and are inverted first. Calcified cartilage has a short T2* and its longitudinal magnetization is not inverted by the adiabatic inversion pulse. Signal from this tissue component is subsequently detected by the UTE data acquisition. **Figure 5** shows clinical and UTE MR imaging of a patella slice from a human cadaver knee specimen. The clinical proton density (PD) weighted (Fig 5A) and T1 fast spin echo (FSE) weighted (Fig 5B) sequences show a signal void for calcified cartilage. The conventional UTE sequence shows high signal for calcified cartilage (Fig 5C), but with limited contrast between it and the superficial layers of cartilage and marrow fat. The DIR-UTE sequence selectively suppresses signals from both marrow fat and the more superficial layers of cartilage, leaving calcified cartilage depicted with high contrast (Fig 5D). An association between signal reduction and increase in thickness in calcified cartilage was observed in the lateral part of the patella (red arrows in Fig 5C and 5D).

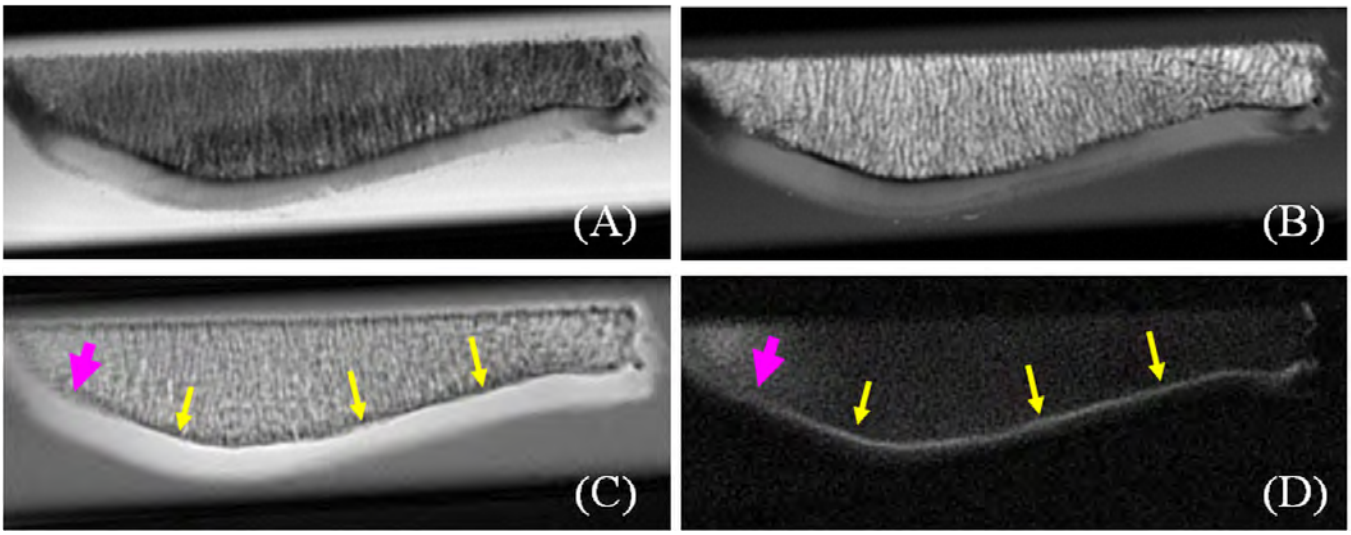

Figure 5. Imaging of a patella slab using PD-FSE (A), T1-FSE (B), regular UTE (C) and DIR-UTE (D) sequences, respectively. The clinical FSE sequences show a signal void for calcified cartilage (A, B). The regular UTE sequence shows high signal for calcified cartilage, but provides little contrast between calcified cartilage (arrows) and the more superficial layers of cartilage (C). The DIR-UTE sequence selectively suppresses signals from fat and the superficial layers of cartilage, providing high contrast depiction of calcified cartilage which is seen as a linear, well-defined area of high signal (thin arrows) (D). There is a reduction in signal and increase in thickness from calcified cartilage in the lateral part of the patella (thick arrows) where morphological degradation was observed.

4.1.3 SWIFT Imaging of Articular Cartilage

Sweep imaging with Fourier transformation (SWIFT) is a different type of very short TE imaging technique [24]. With SWIFT signals are acquired in a time shared manner during a swept RF excitation of the spins with a minimal delay between RF excitation and data acquisition. This technique has considerable potential for imaging objects with spins that have extremely short T2s, such as calcified cartilage and collagen protons [25]. MSK imaging is one of the fields likely to benefit from the sequences capable of detecting nearly all spins, regardless of their T2 values. An example of short T2 saturation and visualization using an MLEV-4 MP block pulse is shown in **Figure 6**. The normal SWIFT image shows a faint line of high intensity in the region of the calcified layer of the cartilage (Fig 6a). After preferential saturation of short T2 components, the bright feature disappears in the image with T2 contrast (Fig 6b). The signals from tissues with short T2 spins can be better visualized by subtracting the saturated image from the SWIFT image. In this image, the bright line at the interface is even more prominent (Fig 6c).

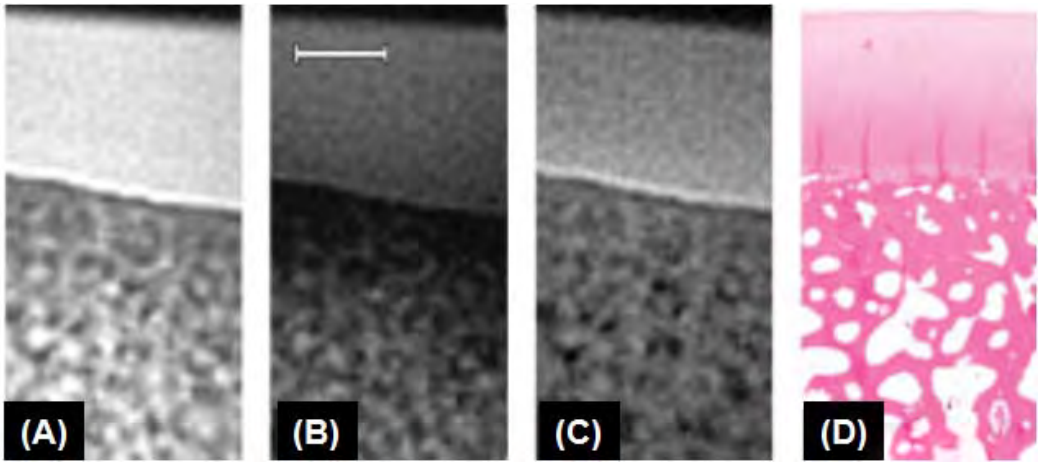

Figure 6 Selected slices from a SWIFT image of a bone-cartilage specimen from an 18-month old pig, acquired at 9.4 T. (a) Normal SWIFT image; (b) SWIFT image with short T2 spins saturated, (c) subtraction image to reveal the short T2 fraction, and (d) Safranin-O stained microscopic image of the same specimen. Scale bar indicates 1 mm. Acquisition parameters were bandwidth = 125 kHz, total number of views = 256 000, isotropic resolution of 65 μm3, scan time ~ 22 min/dataset (20 ms MP block every 16 views).

4.2 Quantitative UTE Imaging of Calcified Cartilage

4.2.1 T1 quantification of calcified cartilage

Quantification of the T1 of calcified cartilage is challenging due to the fast decay of signals from this tissue. Conventional inversion recovery techniques are not useful because it is very difficult to invert the longitudinal magnetization of short T2* tissues or tissue components. They experience significant transverse relaxation during the inversion process. The T1 of calcified cartilage can be measured with different techniques, including saturation recovery UTE imaging, UTE imaging with variable TRs, and UTE imaging with variable flip angles.

It is possible to saturate the short T2 components as well as the long T2 components with a non-selective short duration pulse, allowing T1 quantification of calcified cartilage with a saturation recovery UTE acquisition. In saturation recovery UTE imaging, a short 90^0 square pulse is used in conjunction with large dephasing gradients to suppress signals from marrow fat, superficial layers of cartilage and calcified cartilage. UTE acquisitions with progressively increasing saturation recovery times (TSRs) can then be used to detect the recovery of the longitudinal magnetization of cartilage, including that of calcified cartilage. **Figure 7** shows saturation recovery images of a patella sample arranged in order of increasing TSR. As can be observed, at the lowest value of TSR, the intensity of the entire patella is nearly zero, suggesting efficient saturation of the magnetizations of both short and long T2* components. Subsequently, as TSR is increased, the intensity of various tissues increases at a rate dependent on their respective T1 values. Calcified cartilage is defined as a high signal line (thin arrows in

Fig 7D) with excellent image contrast with the superficial layers (thick arrow in Fig 7D) of cartilage and fatty marrow at TSRs of 100 to 700 ms. Calcified cartilage can be seen prominently at TSRs below 200 ms, suggesting a shorter T1 compared to that of fatty bone marrow and the superficial layers of cartilage. A bi-component exponential fit of the saturation recovery curves derived from small ROIs placed over calcified cartilage and the superficial layers of cartilage, respectively, is also shown (Fig 7H and 7I). Excellent fitting can be achieved for both layers, giving a short T1 of 312 ms for calcified cartilage and a long T1 of 1469 ms for the superficial layers of cartilage. In calcified cartilage the short T1 component accounts for about 70% of the signal, with another 30% from the adjacent long T1 component likely to be due to partial volume effect. Mono-exponential fitting was performed for the bone marrow fat, yielding a T1 relaxation time of 367 ± 57 ms, which is consistent with values reported in the literature [26].

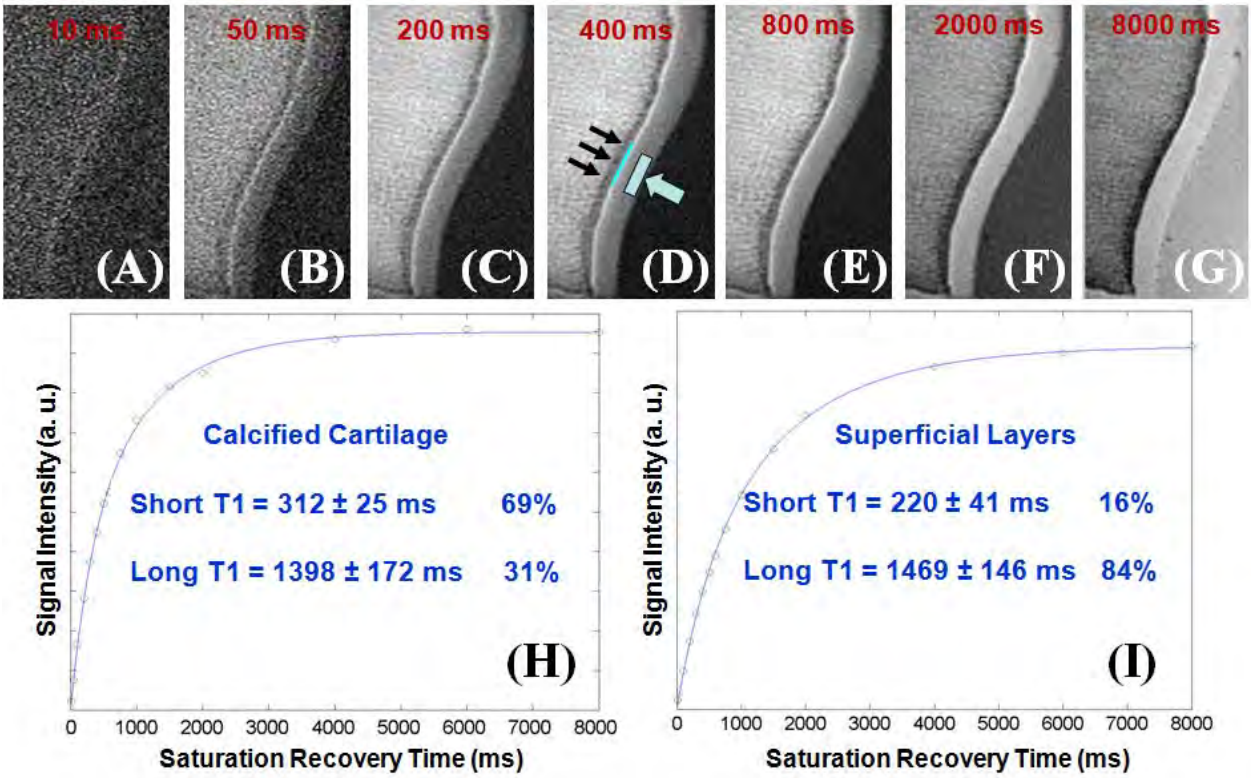

Figure 7 Selected UTE saturation recovery images of a patella sample at TSRs of 10 ms (A), 50 ms (B), 200 ms (C), 400 ms (D), 800 ms (E), 2000 ms (F), 8000 ms (G). Signal from calcified cartilage recovers at a significant faster rate than that from the superficial layers of cartilage, suggesting shorter T1 relaxation time. Bi-component fitting shows that calcified cartilage (thin arrows in D) has a short T1 of 312 ms accounting for 69% of the signal and a long T1 of 1398 ms accounting for 31% of the signal (H). The superficial layers (thick arrow in D) have a long T1 of 1469 ms accounting for 84% of the signal and a short T1 of 220 ms accounting for 16% of the signal. This is likely to be from water bound to proteoglycans and collagen (I).

4.2.2 T2* quantification of calcified cartilage

The DIR-UTE sequence provides robust suppression of long T2 signals, and provides high contrast images of calcified cartilage, which helps with T2* quantification [20]. T2* can be quantified using exponential fitting of DIR-UTE images acquired at a series of TEs. **Figure 8** shows DIR-UTE imaging of calcified cartilage at progressively increasing TEs. The excellent soft tissue suppression from the DIR preparation pulse minimizes signal contamination from the long T2 superficial layers of articular cartilage as well as from marrow fat, resulting in robust measurement of the T2* of calcified cartilage. There is rapid signal decay with increasing TE, suggesting a short T2* relaxation time for calcified cartilage. This is confirmed by the mono-exponential fitting which shows a T2* of 1.79 ± 0.20 ms for calcified cartilage.

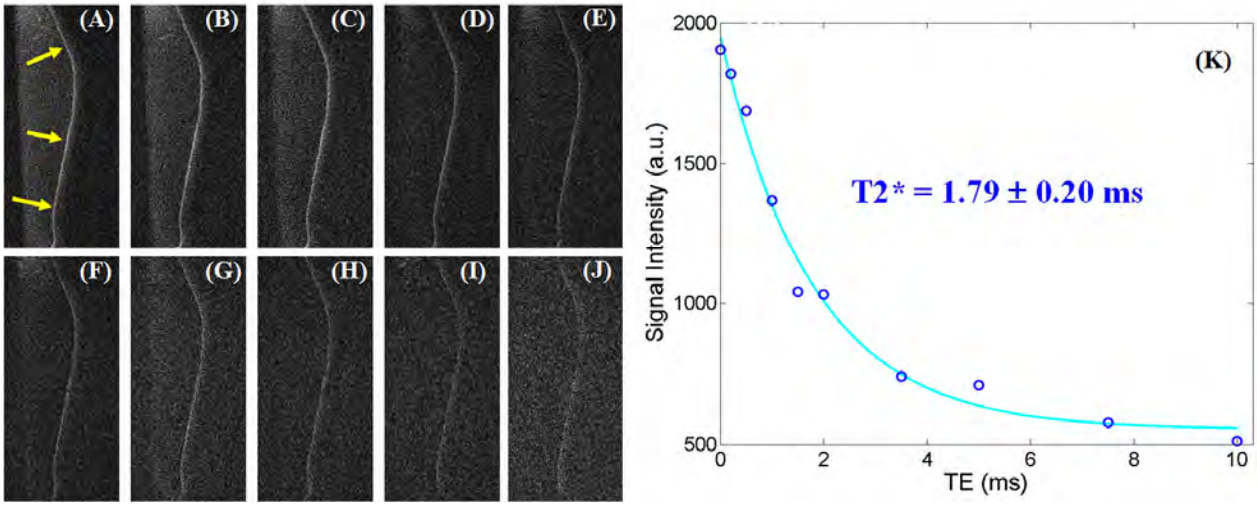

Figure 8. DIR-UTE imaging of calcified cartilage at a series of TEs of 8 µs (A), 200 µs (B), 500 µs (C), 1 ms (D), 1.5 ms (E), 2 ms (F), 3.5 ms (G), 5 ms (H), 7.5 ms (I), 10 ms (J), as well as single component exponential fitting to the decay curve (K). There is loss of signal with increasing TE (A-J). The decay curve (K) shows a short T2* of 1.79 ms for calcified cartilage.

4.2.3 T1rho quantification of calcified cartilage

There are several MR techniques which are of value for detecting PG loss and/or collagen degradation in articular cartilage, including T2 mapping, delayed gadolinium-enhanced MRI of cartilage (dGEMRIC) [27], sodium MRI [28], and T1rho imaging [29]. T1rho has been proposed as an attractive alternative to probe biochemical change in cartilage. It reflects the slow interactions between motion-restricted water molecules and their local macromolecular environment [29], and provides unique biochemical information in the low frequency range from a few hundred Hz to a few kHz. Changes to the extracellular matrix (ECM), such as PG loss and collagen degradation, may be reflected in measurements of T1rho and T1rho dispersion (T1rho values vs. the spin-locking field). Recent studies have demonstrated that T1rho has a high sensitivity to PG loss in bovine cartilage samples as well as to the presence of OA in patients [30].

T1rho of calcified cartilage can be measured with spin-locking prepared DIR-UTE acquisitions at progressively increasing spin-locking times (TSLs) [20]. Quantitative T1rho DIR-UTE imaging of calcified cartilage of a patella sample is shown in **Figure 9**. The DIR-UTE images show calcified cartilage with excellent contrast. It is hardly visible with conventional UTE-T1rho imaging. Exponential fitting of the DIR-UTE images shows a short T1rho of 4.61 ± 0.07 ms, as indicated in Figure 9E.

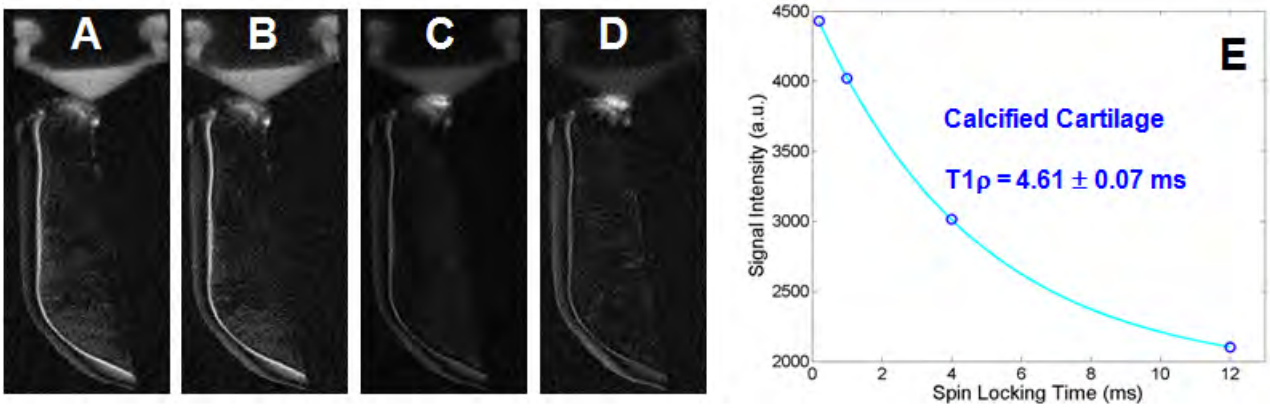

Figure 9. DIR-UTE T1rho imaging of the calcified cartilage at a series of TSLs of 0.02 ms (A), 1 ms (B), 4 ms (C) and 12 ms (D). There is progressive loss of signal from (A) to (D). Single component curve fitting shows a short T1rho of 4.61 ± 0.07 ms (E) for calcified cartilage of this patella.

4.2.4 UTE T2* bi-component analysis of articular cartilage

Biological tissues frequently contain distinct water compartments with different transverse relaxation times (T_{2s}). Clinical techniques for determining multiple components are usually based on exponential fitting data obtained from SE images acquired with Carr-Purcell-Meiboon-Gill (CPMG) sequences. There are three major drawbacks with this approach. Firstly, multi-component fitting is very sensitive to image signal-to-noise ratio (SNR), the number of echoes, the number of fitting components and the difference between T_2 values of the different components. For example, to fit three components plus a noise term it requires a SNR of ~8000 to reduce the fitting error to 2% [31]. This is not achievable with clinical MR imaging. Secondly, clinical CPMG sequences typically have TEs > 10 ms, which may be too long to detect the short T_2 components in commonly studied biological tissues. Thirdly, there is a particular group of biological tissues such as menisci, ligaments, tendons, cortical bone and calcified cartilage which have very short mean T_2s and little or no signal is seen with commonly used clinical SE or GRE sequences [2]. Signal from both short and long T_2 water components in these tissues may be difficult or impossible to detect with conventional approaches.

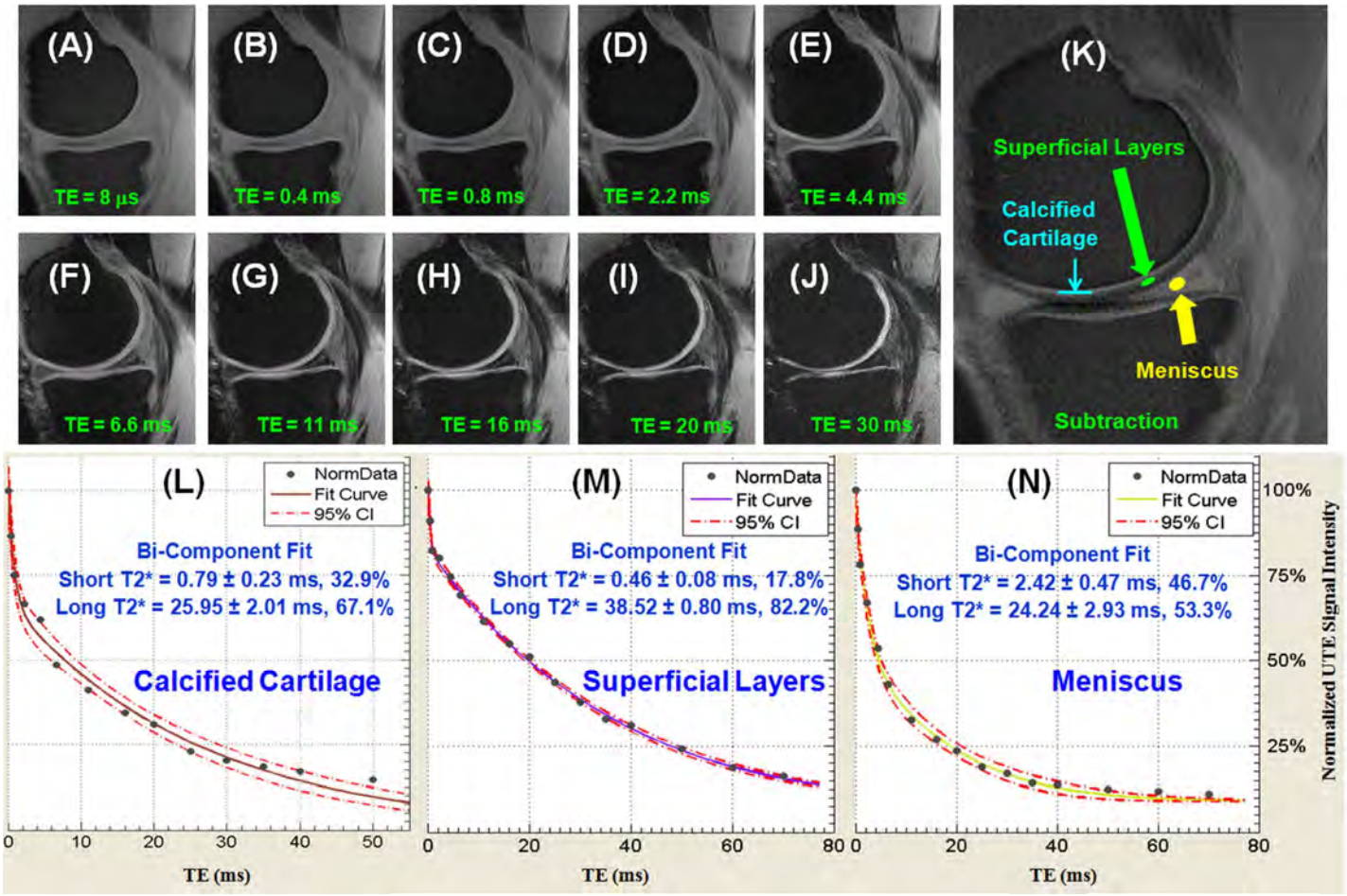

Figure 10. Selected interleaved 4-echo UTE acquisitions with TEs of 8 µs (A), 0.4 ms (B), 0.8 ms (C), 2.2 ms (D), 4.4 ms (E), 6.6 ms (F), 11 ms (G), 16 ms (H), 20 ms (I), 30 ms (J), later echo image subtraction (K), and bi-component T2* analysis for calcified cartilage (L), the more superficial layers of cartilage (M) and meniscus (N). ROIs for calcified cartilage (thin arrow). The more superficial layers of cartilage (long thick arrow) and meniscus (short thick arrow) are shown in (K).

Bi-component T2* analyses of calcified cartilage in vivo is challenging due to the requirement for a long scan time and potential motion artifacts [23]. An interleaved multi-echo UTE acquisition scheme can be employed for fast T2* bi-component analysis of the deep radial and calcified cartilage in healthy volunteers. In this protocol

four sets of four-echo UTE acquisitions with fat suppression were performed with the following imaging parameters: FOV = 14 cm, TR = 200 ms, slice thickness = 3 mm, flip angle = 45°, readout = 320, number of projections = 455, reconstruction matrix = 512×512, four sets of TEs (0.008/4.4/20/40 ms; 0.4/6.6/25/50 ms; 0.8/11/30/60 ms; 2.2/16/35/70 ms), a total scan time of 12 min. **Figure 10** shows UTE T2* imaging of the knee of a 59 year old healthy volunteer. The four sets of four-echo UTE acquisitions cover both short and long T2* ranges, allowing robust estimation of short and long T2* components in the superficial layers of femorotibial cartilage and calcified cartilage as well as the meniscus. Calcified cartilage and the meniscus can be better depicted in the subtraction image (Fig 10K) where a later echo image was subtracted from the first one. The superficial layers of cartilage with longer T2s were effectively suppressed, creating high contrast for calcified cartilage and meniscus. The UTE images were assessed using bi-component analysis at ROIs drawn in the superficial layers of articular cartilage, calcified cartilage and meniscus. These showed excellent curve-fitting, with a short T2* of 0.79 ms (32.9% of the UTE signal) and a longer T2* of 25.95 ms (67.1% of the UTE signal) for calcified cartilage. The longer T2* component is likely from the more superficial layers of cartilage due to partial volume effect. The short and longer T2* values for the superficial layers and meniscus are generally consistent with the values reported in the literature [31, 32].

5. Discussion

It is technically challenging to image bone and bone-tissue interface. Recently developed UTE type sequences can be used to image bone, periosteum and calcified cartilage with high spatial resolution and image contrast. Quantitative evaluation of the different water components and measurement of their MR relaxation times (e.g., T1, T2* and T1rho) are also feasible. However, clinical evaluation of these techniques remain to be done.

References

1. Wehrli FW, Song HK, Saha PK, Wright AC. Quantitative MRI for the assessment of bone structure and function. NMR in Biomed 2006; 19:731-764.
2. Robson MD, Gatehouse PD, Bydder M, Bydder GM. Magnetic resonance: an introduction to ultrashort TE (UTE) imaging. J Comput Assist Tomogr 2003; 27:825-846.
3. Wu Y, Ackerman JL, Chesler DA, Graham L, Wang Y, Glimcher MJ. Density of organic matrix of native mineralized bone measured by water- and fat-suppressed proton projection MRI. Magn Reson Med 2003; 50:59-68.
4. Techawiboonwong A, Song HK, Leonard MB, Wehrli FW. Cortial bone water: in vivo quantification with ultrashort echo-time MR imaging. Radiology 2008; 248:824-833.
5. Du J, Carl M, Bydder M, Takahashi A, Chung CB, Bydder GM. Qualitative and quantitative ultrashort echo time (UTE) imaging of cortical bone. J Magn Reson 2010; 207:304-311.
6. Biswas R, Bae CW, Diaz E, Masuda K, Chung CB, Bydder GM, Du J. Ultrashort echo time (UTE) imaging with bi-component analysis: bound and free water evaluation of bovine cortical bone subject to sequential drying. Bone 2012; 50:749-755.
7. Bae WC, Chen PC, Chung CB, Masuda K, DLima D, Du J. Quantitative ultrashort echo time (UTE) MRI of human cortical bone: correlation with porosity and biomechanical properties. J Bone Miner Res 2012; 27:848-857.
8. Horch R, Gochberg D, Nyman J, Does M. Clinically-compatible MRI strategies for discriminating bound and pore water in cortical bone. Magn Reson Med 2012; 68:1774-1784.
9. Du J, Bydder M, Bydder GM, Chung CB. Ultrashort echo time imaging of periosteum on a clinical 3T magnetic resonance system. RSNA 2007, VS21-04.
10. Bullough PG, Yawitz PS, Tafra L, Boskey AL. Topographical variations in the morphology and biochemistry of adult canine tibial plateau articular cartilage. J Orthop Res. 1985;3:1–16.
11. Recht MP, Resnick D. Magnetic resonance imaging of articular cartilage: an overview. Top Magn Reson Imaging 1998; 9:328-336.
12. Oegema TR, Carpenter RJ, Hofmeister F, Thompson RC. The interaction of the zone of calcified cartilage and subchondral bone in osteoarthritis. Microsc Res Tech 1997; 37:324-332.

13. Mente PL, Lewis JL. Elastic modulus of calcified cartilage is an order of magnitude less than that of subchondral bone. J Orthopaedic Research 1994; 12:637-647.
14. Anderson DD, Brown TD, Radin EL. The influence of basal cartilage calcification on dynamic juxtaarticular stress transmission. Basal Cartilage Calcification 1993; 286:298-307.
15. Burr DB. Anatomy and physiology of the mineralized tissues: role in the pathogenesis of osteoarthrosis. Osteoarthritis and Cartilage 2004; 12:S20-S30.
16. Ferguson VL, Bushby AJ, Boyde A. Nanomechanical properties and mineral concentration in articular calcified cartilage and subchondral bone. J Anat 2003; 203:191-199.
17. Revell PA, Pirie C, Amir G, Rashad, Walker F. Metabolic activity in the calcified zone of cartilage: observations on tetracycline labeled articular cartilage in human osteoarthritic hips. Rheumatol Int 1990; 10:143-147.
18. Miller LM, Novatt JT, Hamerman D, Carlson CS. Alternations in mineral composition observed in osteoarthritic joints of cynomolgus monkeys. Bone 2004; 35:498-506.
19. Du J, Takahashi A, Bae WC, Chung CB, Bydder GM. Dual inversion recovery, ultrashort echo time (DIR UTE) imaging: creating high contrast for short-T2 species. Magn Reson Med 2010; 63:447-455.
20. Du J, Carl M, Bae WC, Statum S, Chang E, Bydder GM, Chung CB. Dual inversion recovery ultrashort echo time (DIR UTE) imaging and quantification of the zone of calcified cartilage. Osteoarthritis Cartilage 2013; 21:77-85.
21. Nissi MS, Lehto LJ, Corum CA, Idiyatullin D, Ellermann JM, Gröhn OH, Nieminen MT. Measurement of T_1 relaxation time of osteochondral specimens using VFA-SWIFT. Magn Reson Med 2014 Aug 8 (Epub ahead of print).
22. Pauli C, Bae WC, Lee M, Lotz M, Bydder GM, DLima D, Chung CB, Du J. Ultrashort echo time (UTE) magnetic resonance imaging of the patella with bi-component analysis: correlation with histopathology and polarized light microscopy. Radiology 2012; 264:484-493.
23. Qian Y, Williams A, Chu CR, Boada FE. Multi-component T2* mapping of knee cartilage: technical feasibility ex vivo. Magn Reson Med 2010; 64:1426-1431.
24. Idiyatullin D, Corum C, Park JY, Garwood M. Fast and quiet MRI using a swept radiofrequency. J Magn Reson 2006; 181:342-349.
25. Rautiainen J, Salo EN, Tiitu V, Finnila MAJ, Aho OM, Saarakkala S, LehenkariP, Ellermann JM, Nissi MJ, Nieminen MT. In: Proceedings of the 21st Annual Meeting of ISMRM, Salt Lake City, USA 2013, p434.
26. Stanisz GJ, Odrobina EE, Pun JH, Escaravage M, Graham SJ, Bronskill MJ, Henkelman RM. T1, T2 relaxation and magnetization transfer in tissue at 3T. Magn Reson Med 2005; 54:507-512.
27. Bashir A, Gray ML, Boutin RD, Burstein D. Glycosaminoglycan in articular cartilage: in vivo assessment with delayed Gd(DTPA)(2-)-enhanced MR imaging. Radiology 1997; 205:551-558.
28. Bashir, A., M.L. Gray, J. Hartke, and D. Burstein, Nondestructive imaging of human cartilage glycosaminoglycan concentration by MRI. Magn Reson Med 1999; 41:857-865.
29. Duvvuri U, K.S., Reddy R, Leigh JS, T1 (rho) relaxation can assess longitudinal proteoglycan loss from articular cartilage in vitro. Osteoarthritis Cartilage 2002; 10:838-844.
30. Li X, Ma B, Link TM, Castillo D, Blumenkrantz G, Lozano J, Carballido-Gamio J, Ries M, Majumdar S. In vivo T1ρ and T2 mapping of articular cartilage in osteoarthritis of the knee using 3T MRI. Osteoarthritis and Cartilage 2007; 15:789-797.
31. Reiter DA, Lin PC, Fishbein KW, Spencer RG. Multicomponent T2 relaxation analysis in cartilage. Magn Reson Med 2009; 61:803-809.
32. Gold GE, Thedens DR, Pauly JM, Fechner KP, Bergman G, Beaulieu CF, Macovski A. MR imaging of articular cartilage of the knee: new methods using ultrashort TEs. AJR Am J Roentgenol. 1998;170:1223–1226.